A study of the monsoonal hydrology contribution using a 8-year record (2010–2018) from superconducting gravimeter OSG-060 at Djougou (Benin, West Africa)

J Hinderer, B. Hector, U. Riccardi, Séverine Rosat, J-P Boy, M. Calvo, F. Littel, J-D Bernard

A study of the monsoonal hydrology contribution using a 8 year record (2010-2018) from superconducting gravimeter OSG-060 at Djougou (Benin, West Africa)

Hinderer[1], J., Hector[2], B., Riccardi[3], U., Rosat[1], S., Boy[1], J.-P., Calvo[4], M., Littel[1], F. & Bernard[1], J.-D.

1 Institut de Physique du Globe de Strasbourg, UMR 7516, CNRS/Université de Strasbourg, France
2 Institut des Géosciences de l'Environnement, Grenoble, France
3 Dipartimento di Scienze della Terra, dell'Ambiente e delle Risorse (DiSTAR), University "Federico II" of Naples, Italy
4 Istituto Geografico National, Madrid, Spain

Abstract

We analyze a nearly 8-year record (2010-2018) of the superconducting gravimeter OSG-060 located at Djougou (Benin, West Africa). After tidal analysis removing all solid Earth and ocean loading tidal contributions and correcting for the long term instrumental drift and atmospheric loading, we obtain a gravity residual signal which is essentially a hydrological signal due to the monsoon. This signal is first compared to several global hydrology models (ERA, GLDAS, MERRA). Our superconducting gravimeter residual signal is also superimposed onto episodic absolute gravity measurements and to space gravimetry GRACE data. A further comparison is done using local hydrological data like soil moisture in the very superficial layer (0-1.2 m), water table depth and rainfall. The temporal evolution of the correlation coefficient between the gravity observation and both the soil moisture and the water table is well explained by the direct infiltration process of rain water together with the lateral transfer discharging the water table.

Finally we compute the water storage changes (WSC) using a simulation based on the physically-based Parflow-CLM numerical model of the catchment, which solves the water and energy budget from the impermeable bedrock to the top of the canopy layer using the 3D Richards equation for the water transfers in the ground, the kinematic wave equation for the surface runoff, and a land surface model (CLM) for the energy budget and evapotranspiration calculation.

This model forced by rain is in agreement with evapotranspiration and stream flow data and leads to simulated water storage changes that nicely fit to the observed gravity signal. This study points out the important role played by surface gravity changes in terms of a reliable proxy for water storage changes occurring in small catchments.

Keywords: time variable gravity, Africa, hydrology, loading, monsoon

Introduction

The superconducting gravimeter OSG-060 from GWR Instruments was installed in Nalohou, close to Djougou in northern Benin (West Africa) in July 2010. This installation was done in the frame of the GHYRAF (Gravity and Hydrology in Africa) program that lasted from 2008 to 2012 (Hinderer et al. 2012). This gravimeter is part of the IGETS (International Geodynamics and Earth Tides Service, (*http://igets.u-strasbg.fr*) (see also Boy et al. 2017), under the umbrella of IAG (International Association of Geodesy).
Fig. 1 shows the location of the Djougou (DJ) station (the geographical coordinates of the station are 9.7424 °N and 1.6056 °E) among the other stations of the international network of superconducting gravimeters (SG).

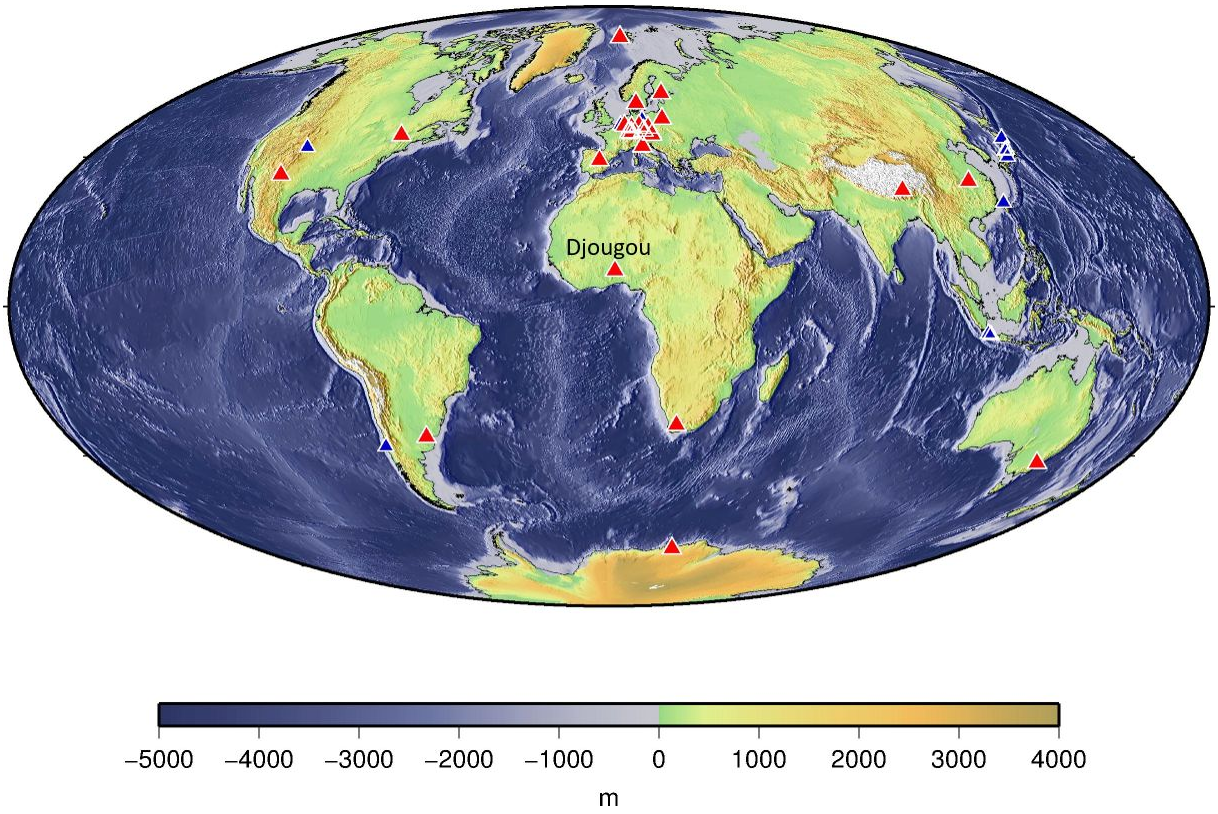

Fig. 1. A map of the superconducting gravimeter stations belonging to IGETS (International Geodynamics and Earth Tides Service, http://igets.u-strasbg.fr). The operational stations in 2018 (about 20) are in red and former stations now stopped are in blue.

The location of Djougou in Benin makes this station unique for investigating the hydrology contribution of the West African monsoon. The choice of this location for installing the SG was driven by the fact that Nalohou is part of the Ara catchment (see Fig. 2) , one of the key sites in the Sudanian region monitored by AMMA-CATCH hydro-meteorological observatory (http://www.amma-catch.org/, AMMA-CATCH, 1990) with a high density of data available over a long time span of several decades (Galle et al. 2018).

The right hand side of Figure 2 (Fig. 2d) shows the location of the various hydro-meteorological instrumentation deployed (piezometers, neutron probe boreholes, rain gauge, Parshall, trenches) over the catchment as well as the gravimeter (FG5, SG-060, CG5) stations and MEP (Multi-electrode Electrical Profiling) profiles. In this study we use an absolute gravimeter FG5#206 from Micro-g Solutions Inc., and a superconducting gravimeter SG-060 from GWR Instruments Inc. .The huts for

episodic absolute gravity measurements (FG5#206) and continuous superconducting gravimeter monitoring (GWR OSG-060) are very close to each other (a few meters) and located on the summital part of the catchment. Since 2011 there is also a network of relative gravity stations that has been regularly repeated with a Scintrex, model CG-5 (serial number 9379) gravimeter.

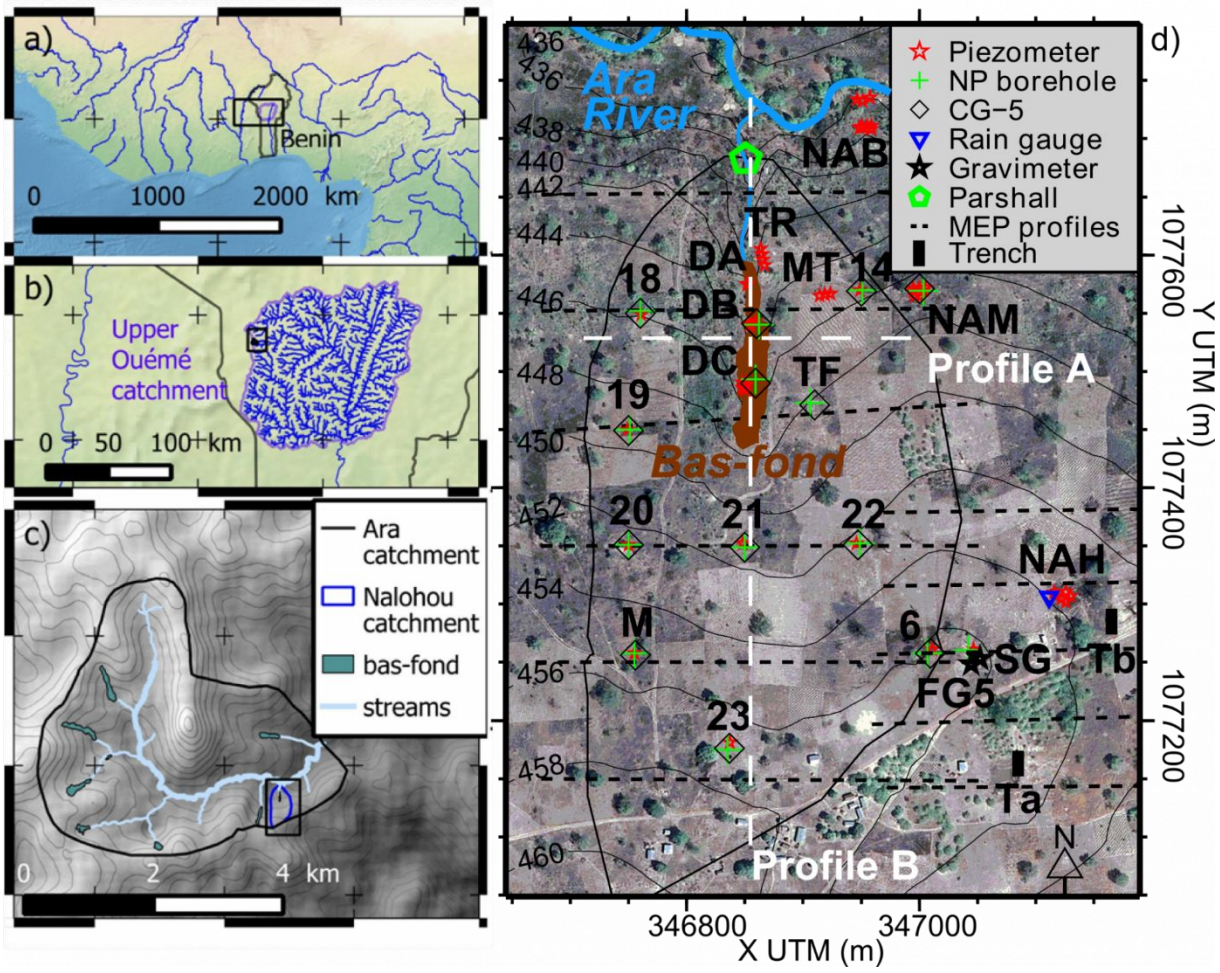

Fig. 2. Location of the Ara catchment inside the Upper Ouémé catchment in North Benin and available hydro-meteorological and geophysical instrumentation (Hector et al. 2015); 2a) shows the upper Ouémé catchment in northern Benin, 2b shows the Ara catchment inside the upper Ouémé catchment, and 2c shows the location of the Nalohou catchment inside the Ara catchment. 2d) indicates all available instrumentation in hydrology and geophysics in the Nalohou catchment (WGS 84 / *UTM* zone *31N* projected coordinate system). *NP means Neutron probe, MEP Multi-electrode Electrical Profiling, Parshall a Parshall flume for measuring the flow of water and Bas-Fond is the French and local name for an inland valley wetland.*

Fig. 3. A picture of the absolute gravimeter FG5#206 (left) and superconducting gravimeter GWR OSG-060 (right) operating at Djougou.

The main goal of installing an SG in Djougou was to monitor integrated water storage changes (WSC) in the sensitivity zone around the gravimeter by observing temporal gravity changes and compare them with point-scale hydrological measurements, such as water table depth, soil moisture sensors, or neutron probe monitoring.

There are several reasons to estimate water storage changes (WSC):

- To observe non-invasively a signature of the internal redistribution of water within the critical zone for hydrological processes identification (proxy)
- To provide additional constraints for hydrological modeling
- To inform ultimately on groundwater recharge and annual storage/discharge that is critical for resource managers.

The question of the hydrological signature in gravity has been extensively studied by many groups possessing superconducting gravimeters. It would be long to cite them all and we refer the reader to the review done in Hinderer et al. (2015), as well as in the more recent one by Van Camp et al. (2017). These studies mostly concern Europe (e.g. Creutzfeld et al. 2010; Weise and Jahr, 2018; Van Camp et al. 2006; Boy and Hinderer 2006) and hence the Djougou station is interesting by its unique location in Africa and because the investigation of monsoonal effects in West Africa has shown a clear intensification of rainfall and hydrological cycles that might be linked to climate changes (see Taylor et al. 2017; Galle et al. 2018, Nkrumah et al., 2019).

Gravity data processing

The gravity record has been processed jointly with air-pressure in a classical way starting with a pre-processing to remove the major disturbances (spikes, offsets, gaps, offsets) of instrumental and/or manmade origin. We refer the reader to Hinderer et al. (2015) for more details on the processing steps.

The gaps due to earthquakes are filled with a synthetic local tide coming from a precise tidal analysis of the 8-year data set (Hinderer et al. 2019).

The cleaned pressure and gravity data sets are shown on Fig. 4 for the investigated period (2010-2018). The reduction for lunisolar tides (solid Earth + ocean tidal loading), as well as for atmospheric effects and Earth's rotation leads to the gravity residuals (in black on Fig. 5). We refer the reader to Hinderer

et al. (2019) for more details on the solid Earth tidal model as well as on the ocean tidal model and atmospheric corrections for the OSG-060 gravity record.

A further correction for the instrumental drift of the gravimeter (in red on Fig. 5) leads then to the corrected residual signal (in blue on Fig. 5) that is reportedly of hydrological origin and characterized by an annual periodicity (see Hector et al. 2014).

The drift assessment through least-square fitting shows that the instrumental drift of the GWR OSG-060 is composed of an initial exponential term followed by a linear term that remains stable over the years. This is very classical for SGs and confirms the earlier results based on a 1.5 year record of SG-060 (Hinderer et al. 2014a).

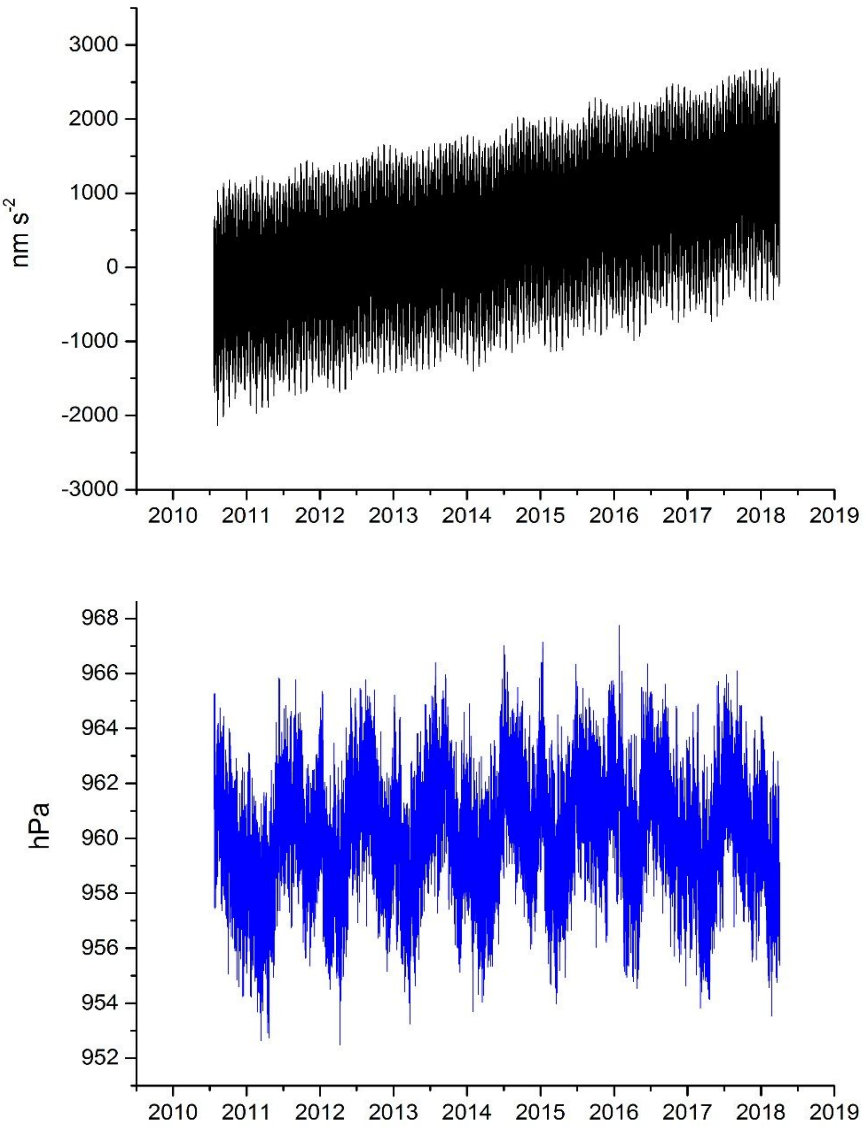

Fig. 4. Gravity (upper panel, in nm s^{-2}) and barometric pressure (lower panel, in hPa) observed at the Djougou station from 2010 to 2018.

The fit to an exponential function $g = g_0 + A_1*\exp(-(x-x_0)/T_1)$, where g_0 and x_0 are the starting values of gravity and time, leads to an amplitude A_1 of -147.6 ± 1.2 nm s^{-2} and a time decay T_1 = 13.8 ± 0.3 days. This exponential drift estimate was done on the residual gravity first corrected for MERRA global hydrology model (Reichle et al. 2017) (see below for this choice) because this contribution mixes up with the instrumental part and must be removed. MERRA model is here the version 2 of The Modern-Era Retrospective analysis for Research and Applications. This hydrology model is available at the EOST loading service (http://loading.u-strasbg.fr). The linear drift is + 213.6 ± 0.1 nm s^{-2}/year which is rather large for SGs (Hinderer et al., 2015), but linearity is very strong and apparently stable in time from our tests.

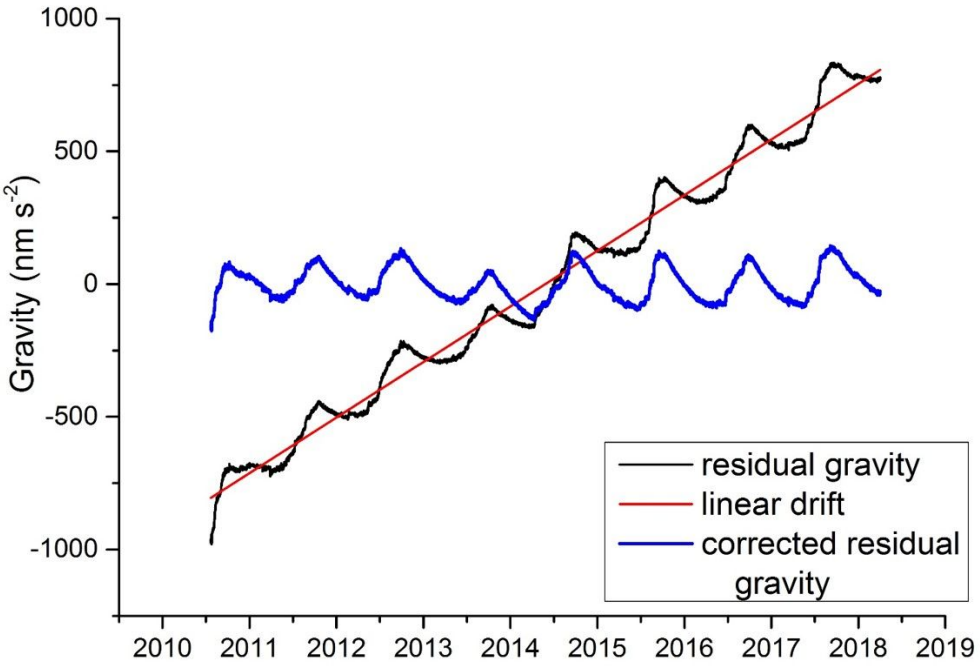

Fig. 5. Residual gravity signal (in black) after correction for solid Earth and ocean tidal loading, atmospheric effects and Earth's rotation; corrected gravity residuals (in blue) after subtracting a linear instrumental drift (in red).

Solid Earth tides, ocean tidal loading and atmospheric loading

We analyzed the whole dataset of gravity observations (nearly 8 years) using the Hartmann & Wenzel (1995) tidal potential catalogue. Amplitude and phase tidal parameters for groups combining inseparable constituents as well as the air pressure admittance factors were adjusted in the long period, diurnal and sub-diurnal frequency bands by means of ET34-ANA v7.1 software (Schüller 2018; Ducarme & Schüller 2018). A detailed discussion of the tidal (solid Earth + oceans) effects, as well as the atmospheric contribution to gravity, is done in Hinderer et al. (2019).

The equatorial location of Djougou station leads to strong pressure waves of thermal origin modulated in amplitude (e.g. Gegout et al. 1998; Schindelegger & Ray 2014). The air pressure also exhibits long period features among which the annual component Sa (one cycle per year) is the largest and the other terms are at Ssa (2 cycle per year) and Sta (3 cycle per year).

The gravity loading due to atmospheric pressure at Djougou takes into account the gravitational attraction of the air masses as well as the elastic deformation of the Earth and hence cannot be reduced to a simple function of the local pressure like in the frame of the classical concept of barometric admittance (Crossley et al. 1995; Hinderer et al. 2014b) but is more complicated because the non-local part involves the convolution of the pressure field worldwide with the atmospheric loading Green's function (see e.g. Boy et al. 2002, 2006).

Different atmospheric gravity loadings were computed using ECMWF (European Centre for Medium Range Weather Forecasts) operational and reanalysis (ERA interim) pressure data, assuming either an inverted barometer response of the oceans (without any induced pressure effect at the ocean bottom see e.g. Wunsch & Stammer 1997) or a dynamic response using TUGO-m (Carrère & Lyard, 2003). The best pressure reduction was found using an hybrid approach computed by retaining the MERRA modelled non-local component and replacing the local one with the observed air pressure multiplied by the nominal admittance coefficient coherently with model resolution. In the MERRA model the resolution is 0.625 ° and we used a local cell with a radius of 0.1 ° together with a nominal admittance of $-2.21\ \mathrm{nm.s^{-2}/hPa}$. The hybrid method enabled us to account for both very local atmospheric effects, as probed by the surface pressure observations, and larger scale contributions to gravity originating from the planetary thermal pressure waves.

Hydrological loading

There are several global hydrology models available at http://loading.u-strasbg.fr. In this study we used GLDAS/Noah [Rodell et al., 2004], ECMWF operational and reanalysis (ERA interim) and MERRA2 [Reichle 2012; Reichle et al., 2017]. Global hydrology models are based on a land surface model (for example, Noah for GLDAS) forced by atmospheric parameters, such as precipitation, temperature, long and short wavelength radiations, etc. They can be run fully coupled with an atmospheric model in case of the ERA interim and MERRA2 reanalysis, or independently as for GLDAS using variables from various origins (atmospheric model, satellite data, etc.). The other main discrepancy is the difference between operational and reanalysis model. In the first case, the model and/or the forcing can change in time, whereas the entire system is stable for reanalysis.

All the hydrology models used in this study are providing estimates of soil moisture content in the first meters, and also canopy water in the case of GLDAS/Noah. We compare all these different models as they can show some discrepancies (see Figure 6), due to differences in the land surface models, but also in the forcings.

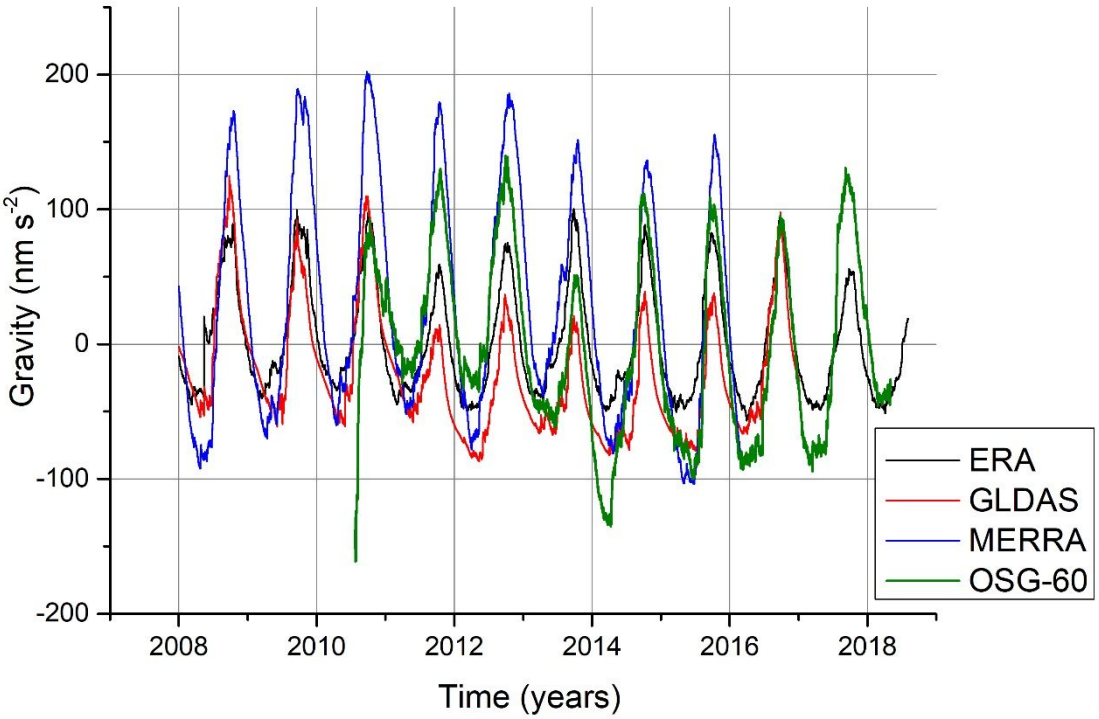

Fig. 6. Comparison of gravity changes due to hydrology according to global models (ERA, GLDAS, MERRA2) with superconducting gravity residuals at Djougou.

For sake of comparison gravity loading from these three hydrology models, computed for the period 2008-2018, are superimposed onto the SG gravity residuals (Fig. 6), which are only available after July 2010 (installation of gravimeter). The beginning of the SG residuals in summer 2010 is clearly different from the hydrology predictions because of the initial instrumental drift of the SG after installation.

By computing the discrepancy between the observed gravity and the hydrology models we are able to find out the preferred model that leads to the best fit. This is shown by the histograms in Fig. 7 depicting the differences between gravity observations and model predictions. The RMS is 42.9, 40.4, 36.8 and 26.1 nm s^{-2} for models GLDAS/Noah, ERA Interim, ECMWF and MERRA2, respectively. Hence, the best model results to be clearly MERRA2.

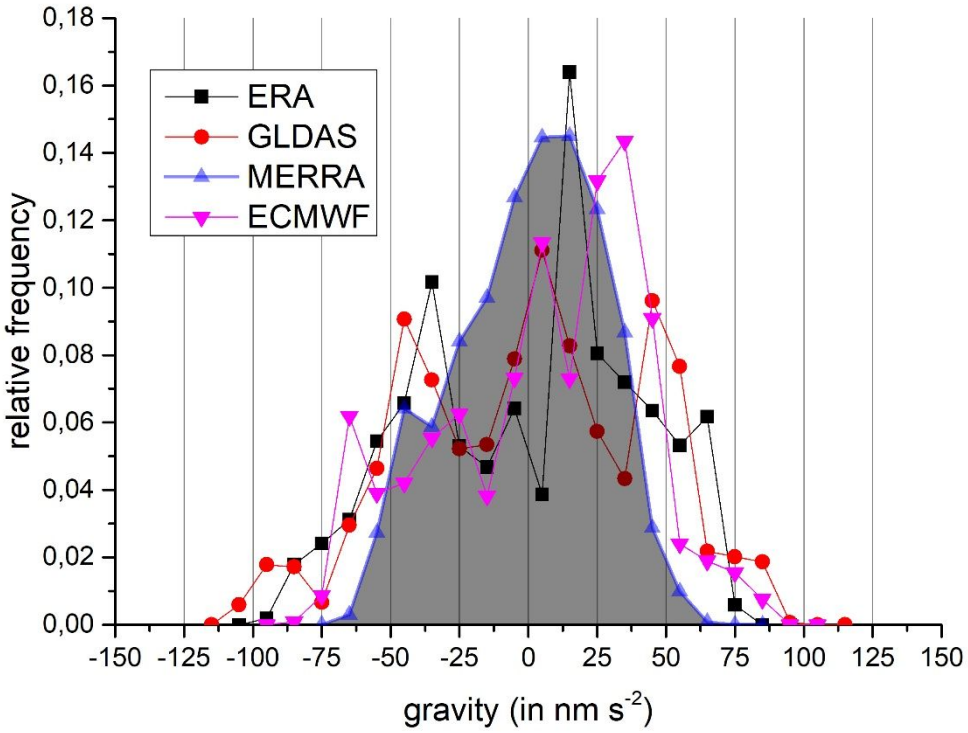

Fig. 7. Histograms of the differences between observed gravity and 4 global hydrology models.

As already shown for shorter duration in previous papers (Hector et al. 2014, 2015), there is a fair agreement between the continuous superconducting gravimeter observations, episodic absolute gravity measurements and space gravimetry GRACE data that all superimpose onto global hydrology models. The comparison of MERRA hydrology model with OSG-060, FG5#206 and GRACE data is shown in Fig. 8 where the GRACE solutions come from iterated global "mascons" (Luthcke et al., 2013).

We use the latest version (v02.4) of the 1-degree equal area global iterated "mascon" solution provided by NASA Goddard Space Flight Center from January 2003 to July 2016. A mascon (mass concentration) represents an excess or a lack of surface mass compared to the a priori mean gravity field in a predefined region, directly inverted from the GRACE K-band range rate measurements. The excess or lack of mass is represented as a uniform water layer, expressed in centimeters of equivalent water over this area. These "mascon" solutions differ from the classical constrained or unconstrained spherical harmonic solutions, as they allow to introduce spatial constraints in the inversion of the K-band range rate residuals (Rowlands et al., 2010), and to increase the spatial resolution of the solution, as post-processing filtering is no longer required.

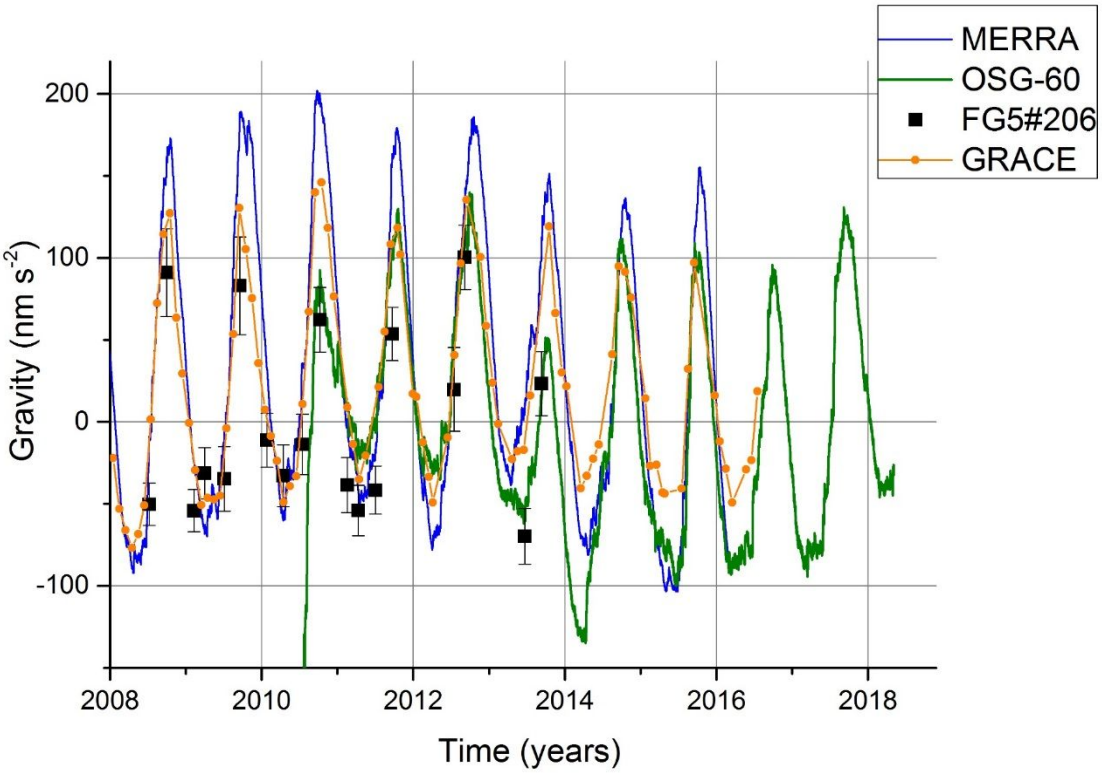

232

233 *Fig. 8. Comparison of MERRA2 hydrology model with superconducting gravimeter (OSG-060), absolute*
234 *gravimeter (FG5#206) and GRACE data.*

235

236 One has to keep in mind that the spatial resolution of these data sets is quite different. Surface gravity
237 is a point measurement, MERRA has a 0.625 ° grid resolution and GRACE data merely are
238 representative of much larger scales (typically 300 x 300 km). The fact that there is a fair agreement
239 between surface gravity and GRACE in Fig. 8 mostly comes from the fact that the hydrology loading of
240 monsoonal origin is coherent over a wide region in West Africa, and probably also because of the
241 specific uphill location of the gravimeter.

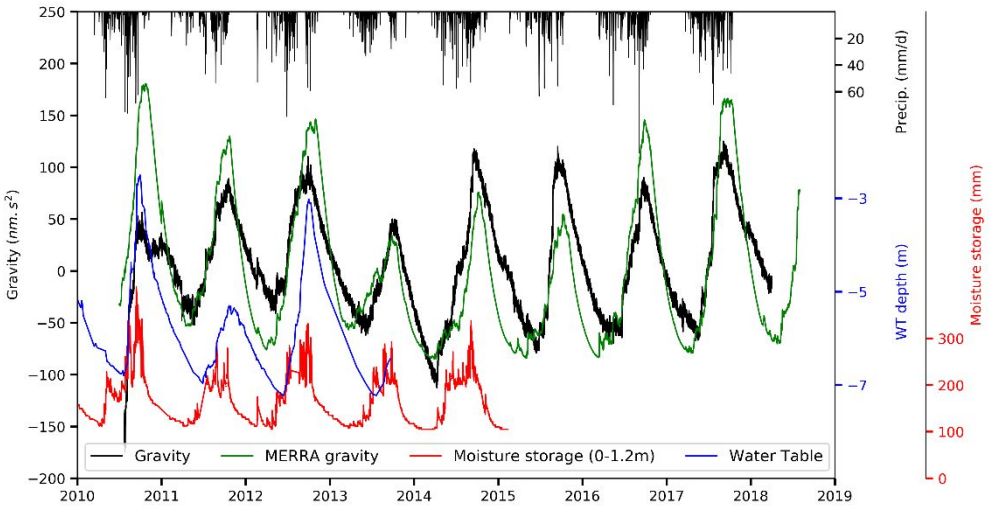

242

Fig. 9. Comparison of gravity observed with the superconducting gravimeter (OSG-060) (black line) and predicted by MERRA global hydrology model (green line), soil moisture (red line) , water table depth (blue line) and rain data in mm/day.

Our last absolute gravity data unfortunately was measured in 2013 and GRACE data stopped in 2016.

In Fig. 9 we show for the period 2010-2015 the comparison of MERRA hydrology model with gravity (OSG-060) (like in Fig. 8) but superimposed onto local hydrological data such as soil moisture (available between 0 and 1.2m using 6 probes at depths of 5, 10, 20, 40 and 60 cm, AMMA-CATCH, 2005), water table depth(AMMA-CATCH, 2003) and rain data(AMMA-CATCH 1999) in the Ara catchment available from the data base of the AMMA-CATCH observation system (Galle et al., 2018, http://www.amma-catch.org/).

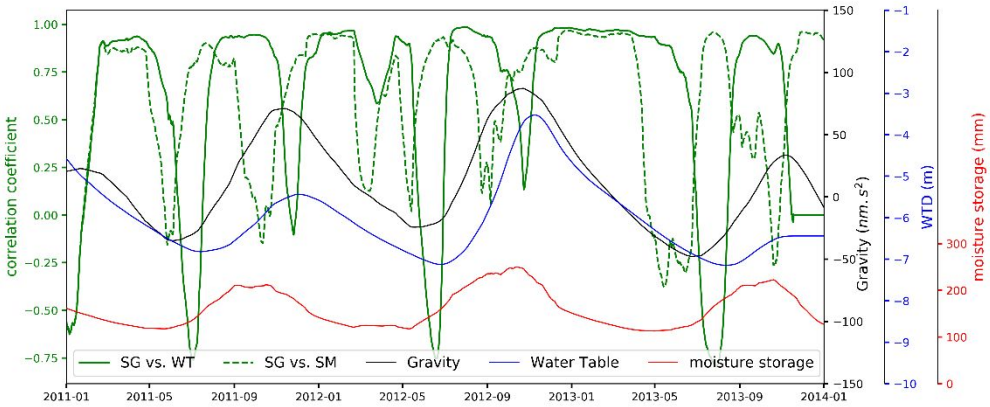

Fig. 10. Correlation coefficient as a function of time between observed gravity (SG) and soil moisture (SM) and water table (WT).

In this ground context, mainly characterized by direct water infiltration, soil moisture reacts more quickly to the rain than the deeper water table. Fig. 10 shows the correlation coefficient computed using a 2-month sliding window (to filter out the higher frequency contributions and keep only the major processes during the hydrological cycle) between SG and both water table and soil moisture. At the onset of the rain season, the level of the water table continues to decrease, the discharge being driven by the hydraulic gradient at the catchment scale (Hector et al., 2015, 2018). This results in a phase lag inducing a decorrelation of the water table and the gravity signal, due to the time offset between the yearly minima of the two series. At the same time, the rain water is being stored in the shallow soil and the correlation between soil storage and gravity takes over until the core of the rainy season, where the soil storage compartment is full (soil moisture time variability shows a plateau), while still maintaining a downward infiltration flux, recharging the water table and increasing the gravity. Thereafter the gravity correlates well to the water table, until the end of the rainy season, where gravity starts to decrease due to the system discharge by evapotranspiration, while the water table still rises in response to the slowly percolating water. During the core of the dry season, all the system discharges and both water table heights and soil moisture values are well correlated to gravity.

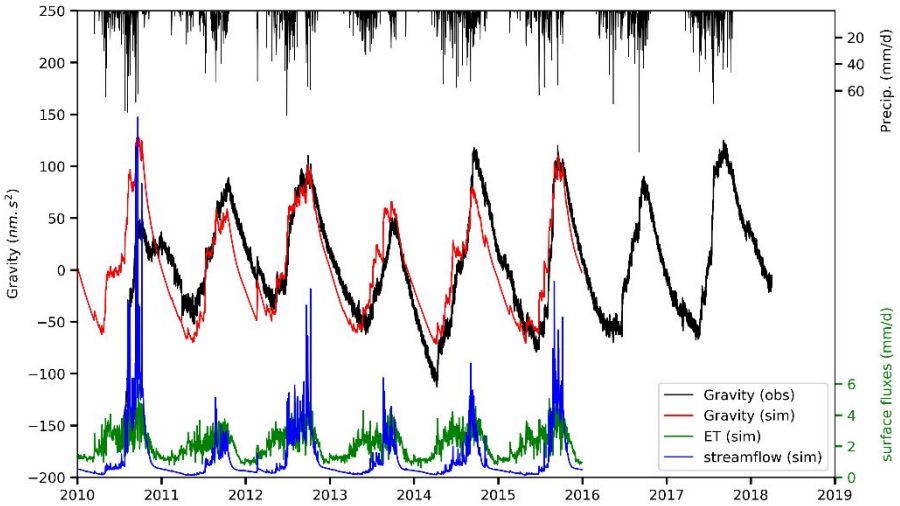

Fig. 11. Modeling the WSC using a simulation of evapotranspiration (ET), streamflow and induced gravity effect based on Parflow-CLM model (Hector et al. 2018) and its validation through the observed gravity.

This means that the transfer function between gravity and water storage changes is variable in time because several processes occur in the water table and soil moisture during the hydrological cycle driven by the monsoon; moreover the WSC are not uniform over the entire catchment as already shown by the analysis of the repeated microgravimetric network observations that could identify zones with preferential infiltration (Hector et al. 2015).

Finally in Fig. 11, the observed gravity is superimposed onto the WSC originating from a simulation (Hector et al. 2018) of a small headwater catchment (720 m x 300 m) encompassing the Nalohou catchment (Fig. 2) with the help of the physically-based critical zone model ParFlow-CLM (Maxwell & Miller 2005; Kollet & Maxwell 2008) run at a 20 m lateral resolution. ParFlow solves the water transfer in porous media on a gridded domain using the 3D Richards equation for the saturated and non-saturated zone, and simultaneously solves the overland flow using the kinematic wave and Manning equation on the surface cells which exhibit a positive pressure (Kollet & Maxwell 2006). ParFlow is tightly coupled to CLM, the Common Land Model (Dai et al., 2003, Maxwell & Miller 2005), a land surface model which solves the water and energy budget through the user-defined N first cells.

The ParFlow model is forced at a 0.5hr time step for 11 years with atmospheric and vegetation variables from the AMMA CATCH observational service; further details on the physical parametrization of the model domain as well as on the model set up can be found in Hector et al. (2018). Three additional years are used as compared to the paper by Hector et al. (2018). Simulation outputs have been extensively tested against multiple field data (streamflow, evapotranspiration, soil humidity, water storage). The SG is seated on the South-East edge of the catchment, on a saprolite unit. Therefore, only the saprolite simulation from Hector et al. (2018) is shown on Fig. 11.

As the SG is located on the edge of the simulation domain, no attempt to calculate the gravity effect of the simulated water storage change (WSC) is done. This would have required a finer resolution close to the gravimeter, and the explicit simulation of the shelter effect as described in Deville et al. (2013) or in the detailed study by Reich et al. (2018). Instead, the simulation represents the typical behavior of a small headwater catchment composed by saprolite rock cover, an elementary hydrological unit in the area.

To convert the water storage changes (in mm of water equivalent) to gravity (nm s^{-2}), the best fit (leading to the smallest differences in time between observations and predictions) yields a factor of 0.37 nm s^{-2}/mm that is lower than the classical Bouguer plate coefficient of 0.42 nm.s^{-2}/mm of water for a flat water layer of density 1000 kg/m^3.

This difference cannot be explained by the topography effect, as computed by Hector et al., 2015 (Their Fig. B1), which would imply a slightly higher coefficient of 0.44 nm.s^{-2}/mm. However, this is in accordance with the range of coefficients found when computing the effect of the shelter (Hector et al., 2014, Fig. 5) for an average depth of water storage changes between 2 and 3 meters, in agreement with the actual depth range comprised between the surface and the water table. Furthermore, this value is still higher than the 'rainfall admittance', the mean observed ratio of gravity increase over precipitation amount computed from a representative diversity of individual rain events, of 0.22 nm.s^{-2}/mm. This value is the lower bound for fast water storage changes occurring close to the surface and for which the gravity measurement is very sensitive to the shelter extent and the sensor height above ground (Hector et al., 2014). This observation clearly calls for a higher resolution simulation of the surroundings of the gravimeter, explicitly simulating the shelter effect to be able to calculate directly the gravity effect. Such a model would also require the simulation of the whole catchment to constrain the lateral groundwater flux, responsible for the groundwater discharge.

The simulated water storage changes match to a reasonable extent the observed gravity changes behaviour (R^2 = 0.77), and while the annual cycle and the inter-annual variations are overall satisfying, there are clear discrepancies around specific events. This may encourage the use of the current model as a correction model for data gap-filling, for long term geodetic applications, but not for high frequency signal analysis, for which a higher resolution model, taking into account the local substratum variability in the vicinity of the gravimeter, together with the shelter effect, is needed (see Reich et al. 2019).

Conclusions

We report on an 8-year long continuous gravity monitoring (2010-2018) by the superconducting gravimeter OSG-060 at Djougou (Benin, West Africa). First, a tidal analysis using ET34-ANA v7.1 software enables us to remove the solid Earth tides, ocean tidal loading and Polar motion effects in the gravity record. Atmospheric pressure effects are reduced by means of a hybrid model using the global atmospheric model MERRA everywhere except in in the local zone, where the model pressure was replaced by the observed pressure accounting for the specific admittance factor. The observed residual gravity signal of hydrological origin was then investigated. We first compared this signal to several global hydrology models (ERA, GLDAS, MERRA) and found that the best model (i.e. the one leading to the smallest discrepancy between observations and model) is MERRA2 with a standard deviation of 26.1 nm s^{-2}. The MERRA hydrology model was also compared to absolute gravity data available from 2008 to 2013 and to GRACE mascons solutions between 2008 and 2016 when GRACE data stopped. In a further step, the gravity signal is compared to local hydrological data like soil moisture in the very superficial layer (0-1.2 m), water table depth and rainfall. The temporal evolution of the correlation coefficient between the gravity observation and both the soil moisture and the water table is well explained by the direct infiltration process of rain water together with the lateral transfer discharging the water table. An attempt to model water storage changes was finally done using a simulation based on Parflow-CLM model of the catchment. This model that is forced by rain is in agreement with evapotranspiration and stream flow data and leads to simulated water storage changes. These changes nicely superimpose onto gravity signal using a 0.37 nm s^{-2}/mm conversion factor. The next step will be to use a finer resolution model in the vicinity of the gravimeter, together with the explicit simulation of the shelter effect, in order to accurately simulate the observed gravity changes and use it as a gap-filling support tool.

The long term monitoring of WSC will help identify possible effects of land use intensification currently occurring in the area (lower duration crop rotation cycles, increased use of pesticides resulting in longer periods of soil denudation, village growth...) on groundwater recharge through increase of surface runoff. Furthermore, a major science question still unresolved in the area is whether the observed groundwater discharge during the dry season is driven by evapotranspiration only, or also by deeper drainage through permeable zones like faults. A comparative analysis of the gravity and water table decreases together with local measurements of evapotranspiration may help to further constrain this issue (Descloitres et al., 2011).

Acknowledgments

We acknowledge the financial support of INSU-CNRS for operating SG 060 in Djougou as part of the French Observatory Service (SNO Gravimétrie). The AMMA-CATCH regional observing system (which is part of the OZCAR research infrastructure in critical zones) was set up thanks to an incentive funding of the French Ministry of Research that allowed pooling together of various pre-existing small-scale observing set-ups. The continuity and long-term perennity of the measurements are made possible by continuous IRD funding since 1990 and by continuous CNRS-INSU funding since 2005. All (or most of) the computations presented in this paper were performed using the Froggy platform of the CIMENT infrastructure (https://ciment.ujf-grenoble.fr), which is supported by the Rhône-Alpes region (GRANT CPER07_13 CIRA), the OSUG@2020 labex (reference ANR10 LABX56) and the Equip@Meso project (reference ANR-10-EQPX-29-01) of the programme Investissements d'Avenir supervised by the Agence Nationale pour la Recherche. Special thanks to Théo Ouani (IRD) and Saré for their continuous help on site.

References

AMMA-CATCH (1999): Precipitation dataset (5 minutes rainfall), over the Donga watershed (600 km2), Benin. IRD, CNRS-INSU, OSUG, OMP, OREME. doi:10.17178/AMMA-CATCH.CL.Rain_Od

AMMA-CATCH (2003): Groundwater dataset (water table level), over the Donga watershed (600 km2), Benin. IRD, CNRS-INSU, OSUG, OMP, OREME. doi:10.17178/AMMA-CATCH.CE.Gwat_Odc

AMMA-CATCH (2005): Soil dataset (soil moisture, temperature, and succion profiles),within the Donga watershed (600 km2), Benin. IRD, CNRS-INSU, OSUG, OMP, OREME. doi:10.17178/AMMA-CATCH.CE.SW_Odc

Boy, J.-P., et J. Hinderer, 2006. Study of the seasonal gravity signal in superconducting gravimeter data, J. of Geodyn., 41, 227-233.

Boy J-P, Gegout P, & Hinderer J (2002) Reduction of surface gravity data from global atmospheric pressure loading. Geophys J Int 149: 534–545

Boy, J.-P., Ray, R., & Hinderer, J., 2006. Diurnal atmospheric tide and induced gravity variations. J. Geodyn. 41, 253–258.

Boy, J.-P., Rosat, S., Hinderer, J., Littel, F. (2017): Superconducting Gravimeter Data from Djougou - Level 1. GFZ Data Services. http://doi.org/10.5880/igets.dj.l1.001

Carrère, L., & Lyard, F., 2003. Modeling the barotropic response of the global ocean to atmospheric wind and pressure forcing – comparisons with observations. Geophys. Res. Lett. 30, doi: 10.1029/2002GL016473.

Crossley DJ, Jensen OG, & Hinderer J (1995) Effective barometric admittance and gravity residuals. Phys Earth Planet Int 90:221–241.

Creutzfeldt, B., Güntner, A., Vorogushyn, S., and Merz, B.: The benefits of gravimeter observations for modelling water storage changes at the field scale, Hydrol. Earth Syst. Sci., 14, 1715–1730, https://doi.org/10.5194/hess-14-1715-2010, 2010.

Dai, Y., Zeng, X., Dickinson, R. E., Baker, I., Bonan, G. B., Bosilovich, M. G., Denning, A. S., Dirmeyer, P. A., Houser, P. R., Niu, G., Oleson, K. W., Schlosser, C. A. and Yang, Z.-L.: The Common Land Model, Bulletin of the American Meteorological Society, 84(8), 1013–1023, doi:10.1175/BAMS-84-8-1013, 2003.

Descloitres, M., Séguis, L., Legchenko, A., Wubda, M., Guyot, A. and Cohard, J. M.: The contribution of MRS and resistivity methods to the interpretation of actual evapo-transpiration measurements: a case study in metamorphic context in north Bénin, Near Surface Geophysics, doi:10.3997/1873-0604.2011003, 2011.

Deville, S., Jacob, T., Chery, J. & Champollion, C., 2013. On the impact of topography and building mask on time varying gravity due to local hydrology, *Geophys. J. Int.,* 192, 82–93.

Ducarme, B., & Schueller, K., 2018. Canonical wave grouping as the key to optimal tidal analysis, Bulletin d'Informations Marees Terrestres (BIM), N°150: 12131-12244. ISSN: 0542-6766; http://www.bim-icet.org/

Galle, S. et al. S., 2018. AMMA-CATCH a Critical Zone Observatory in West Africa Monitoring a Region in Transition. *Vadose Zone Journal*, 17 (1), 180062.

Gegout, P., Hinderer, J., Legros, H., Greff, M., & Dehant, V., 1998. Influence of atmospheric pressure on the Free Core Nutation, precession and some forced nutational motions of the Earth. Phys. Earth Planet. Int. 106, 337–351.

Hartmann, T., & Wenzel, H.G., 1995. The HW95 tidal potential catalogue. Geophys. Res. Lett. 22 (24), 3553–3556.

Hector, B., Hinderer J., Séguis L., Boy J.-P., Calvo, M., Descloitres M., Rosat, S., Galle, S., & Riccardi, U., 2014. Hydro-gravimetry in West-Africa: First results from the Djougou (Benin) superconducting gravimeter, Journal of Geodynamics, vol. 80, 34-49., doi.10.1016/j.jog.2014.04.003

Hector, B., Séguis, L., Hinderer, J., Cohard, J.-M., Wubda, M., Descloitres, M., Benarrosh, N., & Boy, J.-P., 2015. Water storage changes as a marker for baseflow generation process in a tropical humid basement catchment: insights from hybrid gravimetry, Water Resour. Res., 51, doi:10.1002/2014WR015773.

Hector, B., Cohard, J.-M., Séguis, L., Galle, S. & Peugeot, C., 2018. Hydrological functioning of West-African inland valleys explored with a critical zone model, Hydrol. Earth Syst. Sci. Discuss., 2018, 1–35, doi:10.5194/hess-2018-219.

Hinderer J, Pfeffer J, Boucher M, Nahmani S, De Linage C, Boy J-P, Genthon P, Seguis L, Favreau G, Bock O et al (2012) Land water storage changes from ground and space geodesy: first results from the GHYRAF (Gravity and Hydrology in Africa) experiment. Pure Appl Geophys 169(8):1391–1410. doi:10.1007/s00024-011-0417-9

Hinderer J, Crossley D, & Warburton R (2015) Superconducting gravimetry, in treatise on geophysics. In: Herring T, Schubert G (eds) Geodesy, vol 3. Elsevier, Elsevier Science Technology, United Kingdom.

Hinderer, J., Rosat, S., Calvo, M., Boy, J.-P., Hector, B., Riccardi, U., & Séguis, L., 2014a. Preliminary results from the Superconducting Gravimeter SG-060 installed in West Africa (Djougou, Benin). In: Rizos, C., Willis, P. (Eds.), Earth on the Edge: Science for a Sustainable Planet, International Association of Geodesy Symposia. Springer, Berlin Heidelberg, pp. 413–419.

Hinderer, J., Hector, B., Boy, J.-P., Riccardi, U., Rosat, S., Calvo, M., & Littel, F., 2014b. A search for atmospheric effects on gravity at different time and space scales. vol. 80, 50-57 doi: 10.1016/j.jog.2014.02.001

Hinderer, J., Riccardi, U., Rosat, S., Boy, J.-P., Hector, B., Calvo, M., Littel, F., &, Bernard, J.-D., 2019. A study of the solid Earth tides, ocean and atmospheric loadings using an 8-year record (2010-2018) from superconducting gravimeter OSG-060 at Djougou (Benin, West Africa),

Journal of Geodynamics, in press.

Kollet, S. J. and Maxwell, R. M.: Integrated surface–groundwater flow modeling: A free-surface overland flow boundary condition in a parallel groundwater flow model, Advances in Water Resources, 29(7), 945–958, doi:10.1016/j.advwatres.2005.08.006, 2006.

Kollet, S.J., & Maxwell, R.M., 2008. Capturing the influence of groundwater dynamics on land surface processes using an integrated, distributed watershed model, Water Resources Research 44 (2).

Luthcke, S.B., T.J. Sabaka, B.D. Loomis, et al., 2013, Antarctica, Greenland and Gulf of Alaska land ice evolution from an iterated GRACE global mascon solution, J. Glac. 59(216), 613-631, doi:10.3189/2013JoG12J147.

Maxwell, R.M. & N.L. Miller, 2005. Development of a coupled land surface and groundwater model, Journal of Hydrometeorology 6(3):233-247.

Nkrumah, F., Vischel, T., Panthou, G., Klutse, N. A. B., Adukpo, D. C. and Diedhiou, A.: Recent Trends in the Daily Rainfall Regime in Southern West Africa, Atmosphere, 10(12), 741, doi:10.3390/atmos10120741, 2019.

Reich, M., Mikolaj, M., Blume, T., & Güntner, A. (2019). Reducing gravity data for the influence of water storage variations beneath observatory buildings. *Geophysics, 1–81.* doi:10.1190/geo2018-0301.1

Reichle, R. H., 2012: The MERRA-Land Data Product. NASA GMAO Office Note 3 (version 1.2), 38 pp. [Available online at https://gmao.gsfc.nasa.gov/pubs/office_notes/.]

Reichle, R.H., C. Draper, Q. Liu, M. Girotto, S. Mahanama, R. Koster, and G. De Lannoy, 2017: Assessment of MERRA-2 land surface hydrology estimates, J. Climate, doi:10.1175/JCLI-D-16-0720.1

Rodell M, Houser PR, Jambor U, Gottschalck J, Mitchell K, Meng C-J, Arsenault K, Cosgrove B, Radakovich J, Bosilovich M, Entin JK, Walker JP, Lohmann D, & Tol, D (2004) The global land data assimilation system. Bull Am Met Soc 85:381–394

Rowlands, D. D., S. B. Luthcke, J. J. McCarthy, S. M. Klosko, D. S. Chinn, F. G. Lemoine, J.-P. Boy and T. J. Sabaka (2010). Global mass flux solutions from GRACE: A comparison of parameter estimation strategies - Mass concentrations versus Stokes coefficients, J. Geophys. Res., 115, B01403, doi: 10.1029/2009JB006546.

Schindelegger, M., & Ray, R., 2014. Surface Pressure Tide Climatologies Deduced from a Quality-Controlled Network of Barometric Observations, Monthly Weather Review, 142, 4872-4888.

Schüller, K., 2018: Theoretical basis for Earth tide analysis and prediction. Manual-01-ET34-X-V71, Surin 2019.

Taylor, C. M., Belušić, D., Guichard, F., Parker, D. J., Vischel, T., Bock, O., Harris, P. P., Janicot, S., Klein, C. and Panthou, G.: Frequency of extreme Sahelian storms tripled since 1982 in satellite observations, Nature, 544(7651), 475–478, doi:10.1038/nature22069, 2017.

Van Camp M., M. Vanclooster, O. Crommen, T. Petermans, K. Verbeeck, B. Meurers, T. van Dam and A. Dassargues, Hydrogeological investigations at the Membach station, Belgium and application to correct long periodic gravity variations, J. Geophys. Res. 111, B10403, doi:10.1029/2006JB004405, 2006.

Van Camp, M., de Viron, O., Watlet, A., Meurers, B., Francis, O. & Caudron, C. (2017). Geophysics from terrestrial time-variable gravity measurements. Reviews of Geophysics, 55, 938–992. https://doi.org/10.1002/2017RG000566

Weise, A. & Jahr, T., 2018. The Improved Hydrological Gravity Model for Moxa Observatory, Germany, Pure Appl. Geophys., 175: 1755. https://doi.org/10.1007/s00024-017-1546-6

Wunsch C., & Stammer D. 1997. Atmospheric loading and the oceanic “inverted barometer” effect.Rev. Geophys.35:79–107